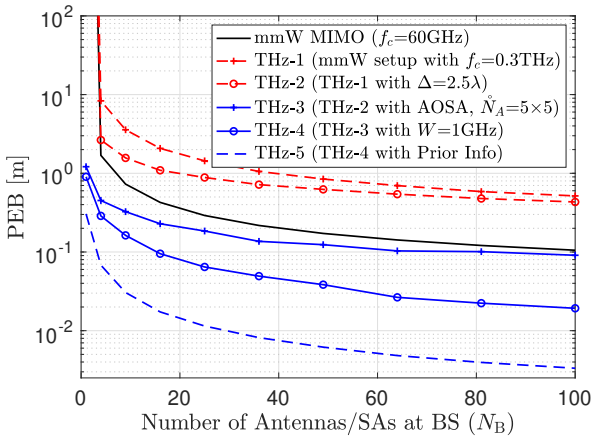

(a) PEB

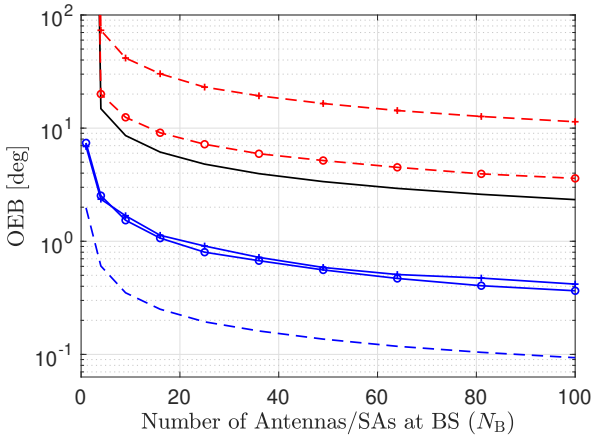

(b) OEB

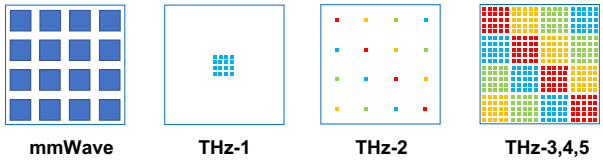

(c) Illustration of different arrays ($N_B = 4 \times 4$)

Fig. 5. PEB/OEB vs. the number of BS antennas/SAs. (a) PEB; (b) OEB; (c) Illustration of different array configurations. By moving the carrier frequency from 60 Ghz to 300 GHz, the error bound increases due to high path losses. Furthermore, increasing the antenna spacing from 0.5λ to 2.5λ (maintaining the same footprint as the mmWave system) improves the performance. Adopting an AOSA structure with an SA size of 5×5 introduces a beamforming gain, and the error bounds outperform the benchmark mmWave system. The bounds can be even lower with a larger bandwidth (1 GHz rather than 100 MHz) and prior information (e.g., setting the beamforming angle of the BS to the direction of a UE).

to be achieved with the same power and footprint compared with mmWave systems. In other words, to achieve the same performance as that of mmWave localization systems, less resources (e.g., power, footprint) are needed. However, to fully exploit the potential of THz localization systems, multiple transmissions and prior knowledge are required to solve the deafness issue. We evaluate the effect of transmission numbers on the CRB in the next subsection.

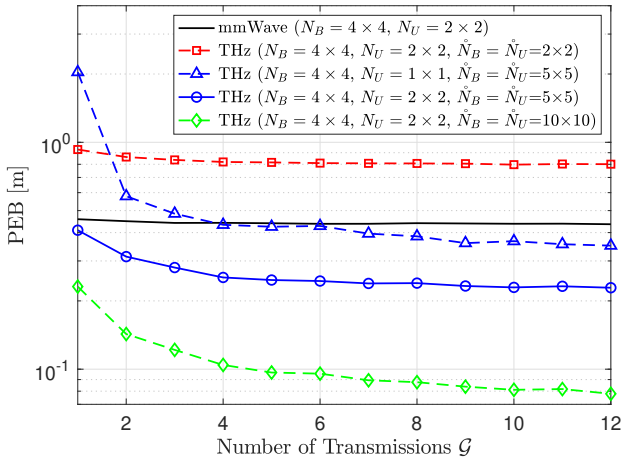

Fig. 6. PEB vs. number of transmissions with a fixed total transmission energy. The number of transmissions has a minor effect on the benchmark mmWave systems. However, multiple transmissions are needed for the AOSA structures adopting analog beamformings, especially when the SA dimension is large. (N is the number of SA, and $\mathring{N}$ is the number of AE per SA.)

B. The Effect of Transmission Numbers on CRB

We simulate the effect of transmission numbers ($\mathcal{G}$) on the PEB with different SA dimensions using fixed total transmission energy and the number of RFCs. Although the AOSA structure can also be adopted in mmWave systems, we use a fully digital array with 4×4 antennas for benchmarking purposes. For THz systems, we simulate different SA dimensions with $\mathring{N}_\mathrm{B} = \mathring{N}_\mathrm{U} = 2 \times 2$, $\mathring{N}_\mathrm{B} = \mathring{N}_\mathrm{U} = 5 \times 5$, and $\mathring{N}_\mathrm{B} = \mathring{N}_\mathrm{U} = 10 \times 10$, respectively. The results are shown in Fig. 6.

We notice that the number of transmissions has a minor effect on the benchmark mmWave systems because of the large beamwidth generated from a small array size. By incorporating the AOSA structures, the computational and hardware cost can be reduced. However, multiple transmissions are needed to obtain a lower bound, where the $\mathcal{G}$ needed for the bound to converge increases with the SA dimension. With more transmissions, the deafness issues can be solved, and a UE can thus be located more accurately. In the next subsection, we discuss the effects of PWM/SWM and Syn/Asyn on the CRB of the system.

C. The Evaluation of PWM/SWM for Different Channel Models

We have discussed several system assumptions, namely synchronized or asynchronized systems (Remark 1), unknown or partially-known channel gains (Remark 2), and SWM/PWM (Sec. III-E1). These assumptions affect the channel realization, system model, and CRB. The PEB for Asyn/Unknown/PWM are not included because the position cannot be estimated in this scenario. For simulation purposes, we assume a single-antenna UE and evaluate the PEBs for different channel models by changing the position of the UE on the x-axis x_U with fixed $y_\mathrm{U} = z_\mathrm{U} = 0$. The simulation results are shown in Fig. 7.

We can see that the boundary between the far-field and near-field is at around 1 m. With the increasing distance, the

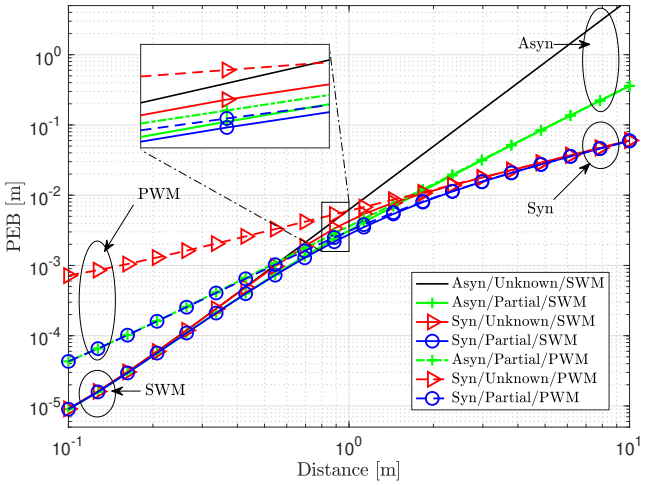

Fig. 7. PEB vs. distance for different localization models assumptions. The PEBs of the systems using different signal models (e.g., SWM and PWM) have a mismatch when the distance from the BS is smaller than 1 m. In addition, a synchronized system performs better, especially when the distance is large.

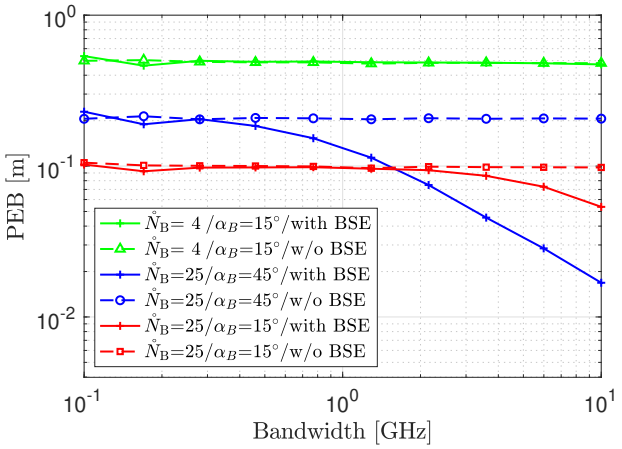

Fig. 8. CRB vs. bandwidth for the systems with/without the beam split effect. The mismatch between different models (solid vs. dashed curves) is larger with increased beamwidth, array size (blue dot vs. green triangle), and angles (blue dot vs. red square).

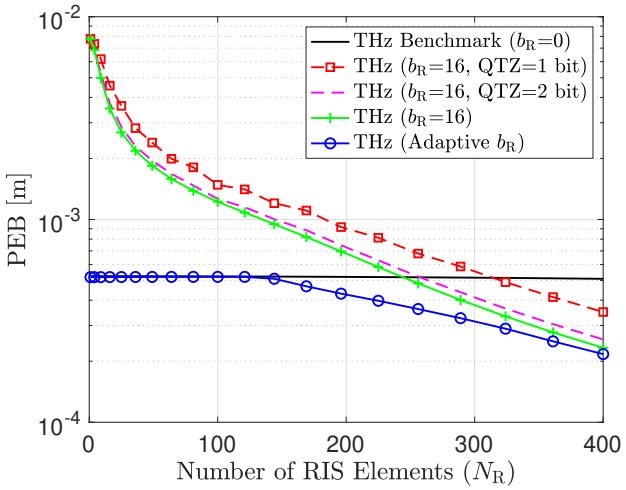

Fig. 9. CRB vs. the number of RIS elements (N_R) for different scenarios ('QTZ' is short for 'quantization'). 'b_R=0' means the SAs at BS/UE are beamforming to UE/BS with prior information; 'b_R=16' indicates all the N_B/N_U SAs at BS/UE are beamforming to the RIS; 'Adaptive' utilizes an optimal beam assignment with grid search).

PEBs of SWM and PWM models are converging. However, the SWM is a more accurate signal model (at the expense of high computational complexity), which is advantageous when the UE is close to the BS. In addition, the SWM can help in synchronization (by exploiting the curvature of arrival) and the PEBs of asynchronized and synchronized systems converge in the near-field.

D. Evaluation of the Beam Split Effect

To evaluate the effect of beam split on the CRB, we assume that prior position information is known, and hence the beamforming angle at the BS is set as pointing to the UE. The orientation of the BS is set as 15° and 45°, and an asynchronized UE is located at $[2, 0, 0]^T$. The PEBs for channel models with and without (w/o) the beam split effect are shown in Fig. 8. Beam split affects the signal gain and is not preferred in communications. However, this 'split' phenomenon may provide extra geometry information (e.g., beams at different subcarriers are pointing to different directions) that can lower the error bound, especially in wide bandwidth systems.

So far, our discussions are limited to LOS channel. In the following, we discuss the effect of RIS and NLOS channels on localization performance.

E. The Effect of RIS on CRB

We simulate the effect of RIS dimensions on the PEB of a THz system. For a better visualization of the convergence, we use scaled positions of BS/RIS/UE as $[0, 0, 0]^T/[0.5, 0.5, 0.1]^T/[0.5, 0.4, 0.05]^T$, and keep other parameters as in Table IX. Assuming prior information is known, the RIS coefficients can be optimized using the method in [70] to maximize the SNR of the received signal. The beamforming angles of each SA at the BS (UE) are set to the directions of either the RIS or UE (BS). For a BS with N_B SAs, the total beams assigned to RIS (b_R) and UE (b_U) satisfies $N_B = b_R + b_U$. Note that such directional beams and SNR-based RIS coefficient optimization is not optimal for localization purposes; however, we use it as a benchmark for further optimization algorithms. Other scenarios also include quantized coefficients (1-bit and 2-bit quantization on the RIS coefficients), and the corresponding simulation results are shown in Fig. 9.

The figure shows that a large RIS with optimized coefficients improves the performance, and a 2-bit quantization on the RIS coefficient is sufficient to assist localization (PEB is close to the setup with continuous phases). Without beamforming to the RIS, an increased number of RIS elements has almost no effect on the PEB of the system. However, with the AOSA structure, the PEB is also affected by the SA beamforming angles (e.g., assigned beams to RIS b_R) and more efforts are needed to jointly optimize active and passive beamforming.

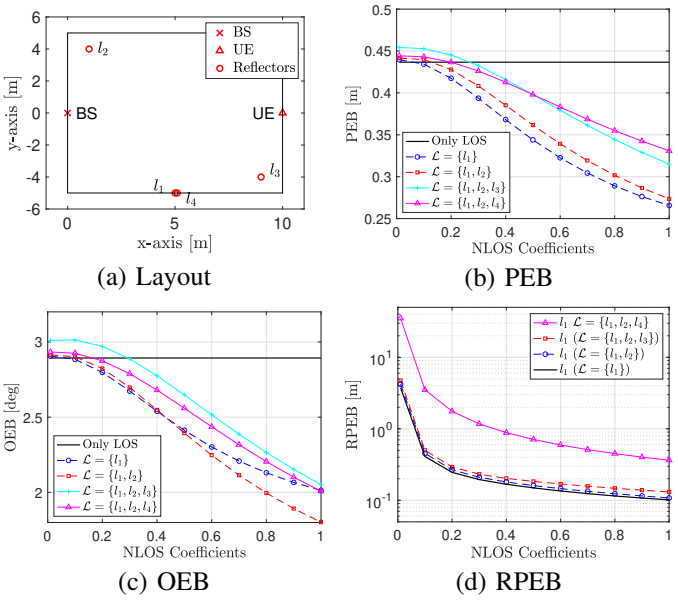

(a) Layout (b) PEB (c) OEB (d) RPEB

Fig. 10. CRB vs. NLOS coefficients. The layout of the BS, UE and possible reflectors is shown in (a), where l_1 and l_4 are not resolvable. The NLOS paths are harmful to the CRB when the reflection coefficients are small. When increasing the coefficients, PEB, OEB, and RPEB get lower. We also notice that even if the positions of the reflectors are not resolvable ($\mathcal{L} = \{l_1, l_2, l_4\}$), the OEB is still lower than in a setup with a weaker NLOS path ($\mathcal{L} = \{l_1, l_2, l_3\}$). However, the RPEB of l_1 in the unresolvable scenario is much higher than in other layouts.

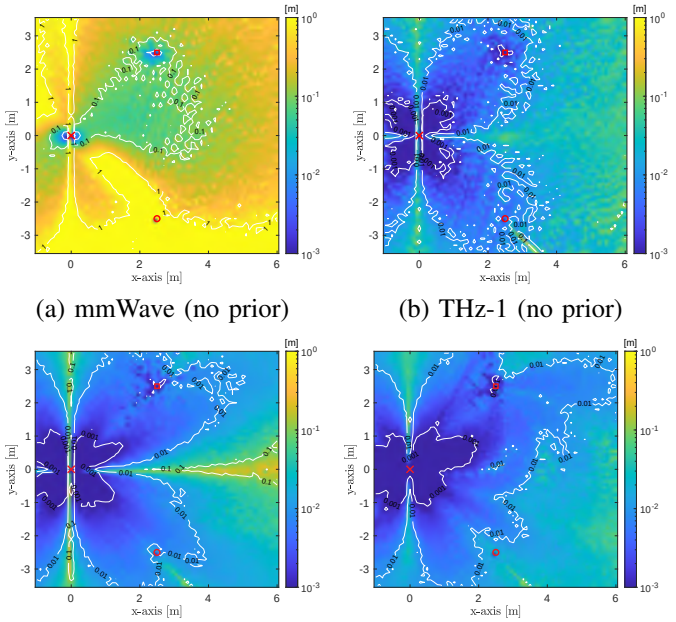

(a) mmWave (no prior) (b) THz-1 (no prior) (c) THz-1 (with prior) (d) THz-2 (with prior)

Fig. 11. 2D PEB visualization for different setups. (a) A conventional 4×4 MIMO system and a 20×20 RIS (5×5 cm footprint); (b) An AOSA-based THz system with 20×20 antennas ($\mathring{N}_{\mathrm{B}} = \mathring{N}_{\mathrm{U}} = 5 \times 5$) and an 100×100 RIS (same footprint as scenario (a)); (c) The same parameters as in (b) are used. By assuming the prior information of the UE position is known, the coefficients of the RIS elements are chosen to maximize the SNR, and 1/4 of the SA beams at the BS/UE are set to point to the RIS; (d) The same setup as (c) THz-1 by changing the UE orientation from $\mathbf{o}_{\mathrm{U}} = [0, 0, 0]^T$ to $\mathbf{o}_{\mathrm{U}} = [5\pi/6, 0, 0]^T$.

F. The Effect of NLOS Paths

We also evaluate the effect of NLOS signals on the CRB with different number of reflectors ($L_N = 0, 1, 2, 3$) as shown in Fig. 10. Four layouts of the landmarks (incident points) are considered, namely, $\{l_1\}$, $\{l_1, l_2\}$, $\{l_1, l_2, l_3\}$ and $\{l_1, l_2, l_4\}$, where l_1-l_4 are located at $[5, -5, 0]^T$, $[1, 4, 0]^T$, $[9, -4, 0]^T$ and $[5.1, -5, 0]^T$, respectively. By changing the reflection coefficients of all the reflectors (assumed to be equal) from 0 to 1, the PEB/OEB of the UE and the reflector position error bound (RPEB) are shown in Fig. 10 (b)-(d).

This figure shows that the NLOS paths are helpful if they are resolvable and the reflection coefficient is large (which depends on the shape and the material of an object). THz channels are expected to have fewer NLOS paths due to the high path loss and narrow beamwidth. With fewer NLOS paths, the number of localization parameters (e.g., the position of reflectors) and non-resolvable paths are reduced. Fewer NLOS paths reduce the computational complexity, but lose geometrical diversity. Hence, more transmission times are needed to improve the localization performance and to map the whole environment.

G. The Visualziation of PEB for Different UE Positions

We visualize the 2D PEB ($z_{\mathrm{U}} = 0$) for different setups by changing the position of UE within a $5 \times 5\,\mathrm{m}^2$ area. The positions of the BS/RIS/reflector are $[0, 0, 0]^T$, $[2.5, 2.5, 0]^T$ and $[2.5, -2.5, 0]^T$, respectively. The number of the BS/UE elements is $N_{\mathrm{B}} = 4 \times 4 / N_{\mathrm{U}} = 2 \times 2$, and the reflection coefficient is set as 0.9. The PEB is obtained with a single snapshot ($\mathcal{G} = 1$), which only works for systems with multiple RFCs.

In Fig. 11 (a) and Fig. 11 (b), the transmitted symbols, beamforming angles, and RIS coefficients are chosen randomly. The THz system generally shows a lower PEB, and even lower PEBs appear when the UE is close to the BS or RIS. Due to the implementation of analog beamforming in the AOSA structure, there exist a 'blind area' in (b) (e.g., $y_{\mathrm{U}} = 0$). In Fig. 11 (c) and Fig. 11 (d), fixed beamforming angles are utilized with prior information. This beam allocation strategy is obviously not optimal, and efficient beamforming optimization algorithms are needed.

H. Summary

In this section, we perform extensive simulations to illustrate the potential of THz systems in localization and sensing. With the incorporation of the RIS, a better localization performance is expected. However, joint optimization of AOSA active beamforming and RIS components is a challenging problem that requires more investigation in the future. Next, we discuss several potential research directions for THz localization, which can assist in algorithm and system design and further improve localization performance.

VII. Lessons Learned and Future Directions

Until now, we have discussed important topics of THz localization and performed extensive simulations with some